Evolutionary Ecology Research, 2000, **2**: 257–277

Habitat selection along an environmental gradient: Theoretical models with an example of Negev Desert rodents

G. Shenbrot* and B. Krasnov

Ramon Science Center, Ben-Gurion University of the Negev, Mizpe Ramon 80600, Israel

ABSTRACT

We present a set of models of density-dependent habitat selection along an environmental gradient. The models are based on the assumption of ideal-free distribution and use an approach similar to Morris' isodar analysis technique. It was assumed that habitats along a gradient differ either qualitatively (efficiency of resource acquisition) or quantitatively (resource abundance) or in both parameters. Depending on the distribution of resource abundance and habitat quality along a gradient, the models predict density-independent or density-dependent habitat distribution with or without density-dependent habitat shifts. The models were tested using data on a desert rodent community of the central Negev Desert, Israel. In six of the nine rodent species (*Gerbillus dasyurus*, *G. gerbillus*, *G. henleyi*, *Meriones crassus*, *Acomys cahirinus* and *A. russatus*), direct estimations of habitat breadth and position fit well the predictions of one of the models based on density relationships. Of these nine species, four (*Jaculus jaculus*, *Gerbillus dasyurus*, *G. gerbillus* and *Mus musculus*) were found to be density-independent habitat selectors, four (*Meriones crassus*, *Psammomys obesus*, *Acomys cahirinus* and *A. russatus*) were density-dependent habitat selectors and one (*Gerbillus henleyi*) was a density-independent habitat selector in winter and a density-dependent habitat selector in summer.

Keywords: density-dependent habitat selection, habitat selection model, Negev Desert, rodents.

INTRODUCTION

The modern theory of habitat selection (Rosenzweig, 1974, 1981, 1989, 1991, 1995) depends on a prediction of single-species, density-dependent habitat selection theory. The latter theory – based on the mechanism of the ideal-free distribution (Fretwell and Lucas, 1970) – predicts a decrease in habitat selectivity as the population density of a single species increases. Indeed, studies of habitat selection in natural populations have shown that such density-dependent habitat selection is quite common. However, density-independent habitat selection has also been reported, albeit infrequently (e.g. Abramsky *et al.*, 1985; Rosenzweig and Abramsky, 1985; Shenbrot and Rogovin, 1995).

Isodar theory (Morris, 1987, 1988, 1990) explains the mechanisms of both density-dependent and density-independent habitat selection and predicts habitat shifts (preference

* Author to whom all correspondence should be addressed.

changes). But isodar theory only analyses habitat selection in a two-habitat system with discrete habitat patches. Many species occur in more than two habitats. Furthermore, often no sharp border separates a pair of habitats in nature. Instead, they occupy two points in a continuum of habitat types. Evolutionary ecology needs to learn how to study and analyse habitat selection along such gradients, which, in essence, contain an infinite number of habitat types.

In this paper, we introduce a method to study habitat selection along such environmental gradients. It will follow the outlines of isodar theory. However, rather than analysing a large number of times and only two habitats, we focus on two times and a large gradient of habitats. Keeping our method in mind, we then develop several models of habitat selection along an environmental gradient, and we test their predictions using a data set taken from Negev Desert rodents.

THE MODEL

The model is based on the following assumptions:

- The habitat distribution of a species is determined mainly by intraspecific competition; interactions with other species play a minor role.
- Habitats differ qualitatively or quantitatively and each species is more efficient at using some habitat types than other habitat types (Rosenzweig, 1989).
- Fitness–density relationships are temporally stable for each habitat type or for each point on a habitat gradient (Morris, 1987, 1988).
- A final, specific assumption helps us to build models that we can test with rodent data: emigration and immigration take place mainly during a short period just after the spring breeding season. This last assumption implies that habitat distribution in all other seasons is at or near the equilibrium, and that density reflects relative habitat suitability.

Consider the following situation. Let individuals of one species inhabit some portion of an environmental gradient. Sample the species' population densities at gradient points at two different times (i.e. at low and high overall densities). If individuals select habitats so as to maximize their net reproductive success, then the density in each habitat will reflect relative habitat suitability. Now we apply an approach similar to isodar theory (Morris, 1987, 1988).

We create a space whose axes are:

- $N_{i,1}$ = density at place i, ($i = a,b, \ldots n$), time 1
- $N_{i,2}$ = density at place i, ($i = a,b, \ldots n$), time 2

We plot the data in this space. Because, from time 1 to time 2, the different places do not change the rank of their suitability, and because the distribution of population at any one time is measured at its equilibrial ideal-free distribution, the data will fall on a monotonically increasing line. We call this line the 'paraisodar'. We will predict the shape of paraisodars from the biology of the species and the nature of the habitat gradient.

Morris (1988) described fitness in habitat i as:

$$\Phi_i = \gamma\left(RA_i - \sum_{n=1}^{N_i} p\,\frac{E_B}{E_i}\right)$$

where Φ_i is expected fitness in i, RA_i is the resource availability in i corrected by its renewal rate, N_i is the number of individuals occupying i, p is per capita demand on resources, E_B/E_i is the efficiency of resource extraction, consumption and conversion into descendants in habitat i relative to the best habitat B, and γ is a scaling constant. In the case of the ideal-free distribution within any given time period, Φ_i is a constant ($\Phi_i = \Phi_j = \phi$ for each i and j).

Model A: Qualitative habitat differences

Suppose that habitats along gradient x differ only qualitatively (i.e. $R(x) = r$ for each value of x), and that efficiency of resource acquisition along the gradient is described by some function $E(x)$ (for example, a Gaussian distribution). This might occur, for instance, if habitat structure directly determines the efficiency of resource acquisition. However it occurs, fitness (Φ) will be the following function of density (N) and efficiency of resource acquisition (E):

$$\Phi(N,E) = \gamma\left(r - N(x)\,\frac{p}{E(x)}\right)$$

Because efficiency is a function of position on the habitat gradient, x, fitness can be described as a function of N and x. Let fitness decrease linearly with an increase of N for each x_i, and let the rate of fitness decrease grow with decreasing efficiency (Fig. 1A). If the ideal-free distribution holds, then, at any given time, Φ_i is a constant ($\Phi_i = \Phi_j = \phi$ for each i and j). For two time periods, 1 and 2, that differ in density:

$$\phi_1 = \gamma\left(r - N_1(x)\,\frac{p}{E(x)}\right)$$

and

$$\phi_2 = \gamma\left(r - N_2(x)\,\frac{p}{E(x)}\right)$$

At both times, $E(x)$ is the same function (because we assumed above that fitness–density relationships are temporally stable), so

$$N_2(x) = bN_1(x)$$

where $b = (\gamma r - \phi_2)/(\gamma r - \phi_1) = N_{\Sigma 2}/N_{\Sigma 1}$. Hence, densities of time 1 plotted against those of time 2 will fall on a straight line with a slope equal to $N_{\Sigma 2}/N_{\Sigma 1}$ and intercept equal to 0 (Fig. 2A).

The following equations determine the position of the habitat centroid (MX):

$$MX_1 = \frac{\sum[xN_1(x)]}{\sum N_1(x)}$$

$$MX_2 = \frac{\sum[xbN_1(x)]}{\sum[bN_1(x)]} = MX_1$$

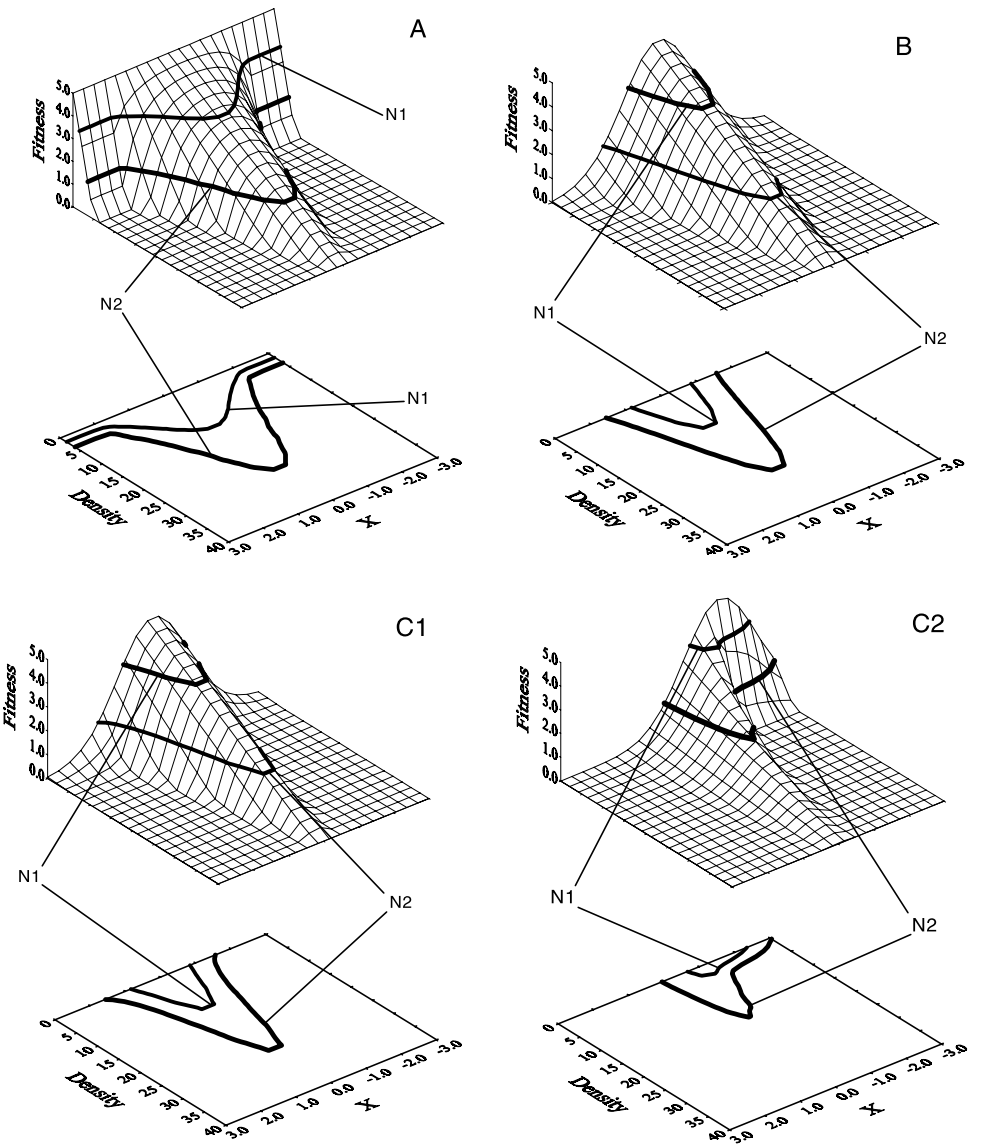

Fig. 1. Three different models of population regulation along an environmental gradient (X) plotted as fitness–density surfaces. Basal projections below surfaces represent density distribution along a gradient at low (N1) and high (N2) density levels. In A, habitats differ qualitatively; in B, habitats differ quantitatively; in C, habitats differ both qualitatively and quantitatively (in C1, the maxima of resource abundance and habitat quality coincide; in C2, the maxima of resource abundance and habitat quality differ).

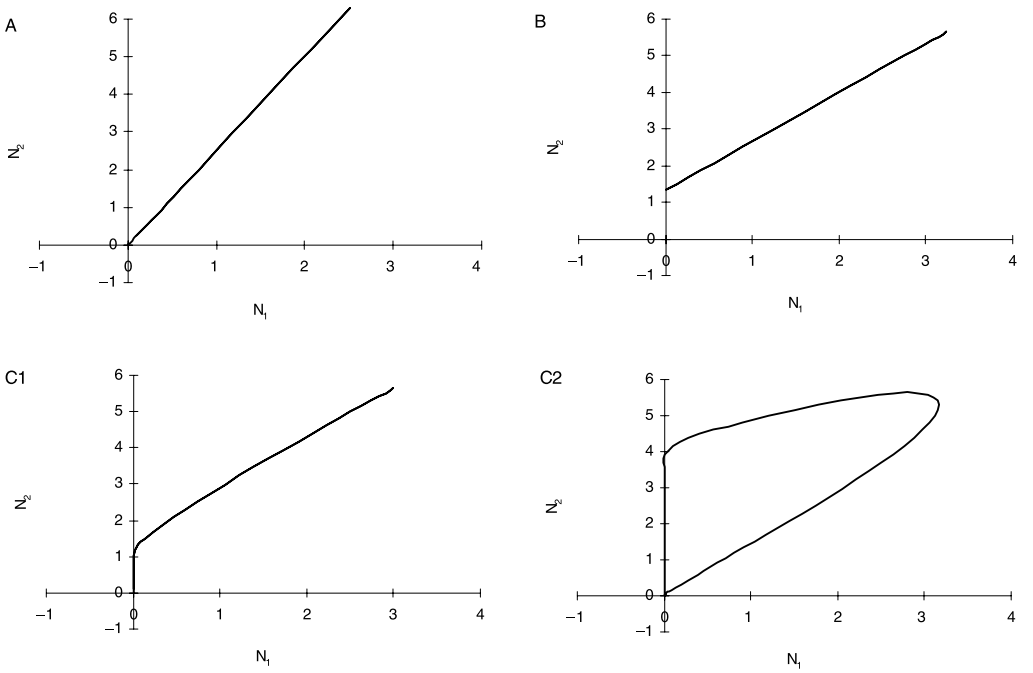

Fig. 2. Habitat paraisodars corresponding to the models of population regulation plotted in Fig. 1. The ordinate is density at high density; the abscissa is density at low density.

The following equations determine habitat breadth (DX):

$$DX_1 = \sqrt{\frac{\sum[(x - MX_1)^2 N_1(x)]}{\sum N_1(x)}}$$

$$DX_2 = \sqrt{\frac{\sum[(x - MX_1)^2 bN_1(x)]}{\sum[bN_1(x)]}} = \sqrt{\frac{b\sum[(x - MX_1)^2 N_1(x)]}{b\sum[N_1(x)]}} = DX_1$$

Thus, the model predicts two stable parameters, namely habitat position and breadth, and it predicts linear density relationships with a regression intercept equal to 0.

Model B: Quantitative habitat differences

Suppose that habitats along a gradient differ only quantitatively (i.e. $E(x) = f$ for each value of x, where E is efficiency, x is habitat position on the gradient and f is a constant), $E_B = 1$ and the shape of resource distribution along this gradient is described by some function R (for example, a Gaussian distribution). In this case, $RA(x) = kR(x)$, where k is a scaling constant for resource abundance, and fitness (Φ) is a function of density (N) and resource abundance (R):

$$\Phi(N,R) = \gamma\left(kR(x) - N(x)\frac{p}{f}\right)$$

Because resource abundance is a function of position on the habitat gradient, x, fitness can be described as a function of N and x. In such a case, fitness decreases linearly at the same rate with an increase of N for each x_i, but the elevation of the fitness–density line decreases with decreasing resource abundance (Fig. 1B). Given an ideal-free distribution within any given time period, Φ_i is a constant ($\Phi_i = \Phi_j = \phi$ for each i and j). For two time periods, 1 and 2, that differ only in density–resource abundance ratio:

$$\phi_1 = \gamma\left(k_1 R(x) - N_1(x)\frac{p}{f}\right)$$

and

$$\phi_2 = \gamma\left(k_2 R(x) - N_2(x)\frac{p}{f}\right)$$

At both times, $R(x)$ is the same function, so

$$\frac{\phi_1}{k_1} + N_1(x)\frac{\gamma p}{f k_1} = \frac{\phi_2}{k_2} + N_2(x)\frac{\gamma p}{f k_2}$$

$$N_2(x) = a + bN_1(x)$$

where $a = (fk_2/\gamma p)((\phi_1/k_1) - (\phi_2 - k_2))$ and $b = k_2/k_1$. Hence, densities of time 1 plotted against those of time 2 will fall on a straight line with a slope equal to k_2/k_1 and an intercept equal to $(fk_2/\gamma p)((\phi_1/k_1) - (\phi_2/k_2))$ (Fig. 2B).

If $k_1 = k_2$, the slope will equal 1 and the position of the habitat centroid (MX) will be:

$$MX_1 = \frac{\sum [xN_1(x)]}{\sum N_1(x)}$$

$$MX_2 = \frac{\sum [xN_2(x)]}{\sum N_2(x)} = \frac{\sum [x(a + bN_1(x))]}{\sum [a + bN_1(x)]} = \frac{\sum xa + b\sum [xN_1(x)]}{\sum a + b\sum [N_1(x)]} \neq MX_1$$

The following equation determines habitat breadth (DX):

$$DX_1 = \sqrt{\frac{\sum [(x - MX_1)^2 N_1(x)]}{\sum N_1(x)}}$$

$$DX_2 = \sqrt{\frac{\sum [(x - MX_2)^2 N_2(x)]}{\sum N_2(x)}} \neq DX_1$$

Now let us assume a Gaussian distribution of resource abundance along the habitat gradient, with $\sigma_R = 1$ and the gradient bounded between -3σ and $+3\sigma$. Inserting these assumptions into our equations relating density (N), habitat breadth (DX) and position (MX), shows that the shape of the relationship between density and habitat position depends on the position of the resource distribution maximum. If the resource maximum coincides with the centre of the gradient, habitat position is stable and density-independent. But if the resource maximum deviates from the centre of the gradient, habitat position shifts from the resource maximum at low density towards the centre of the gradient at high density. Moreover, the extent of this shift increases the further the centre of the gradient is from the value of the resource maximum (Fig. 3A). Habitat breadth increases linearly with

increasing density, and the rate of this growth decreases the further the resource maximum is from the centre of the gradient (Fig. 3B).

Thus, model B predicts a linear density-dependence of habitat position and breadth and linear density relationships with a non-zero regression intercept.

Model C: Combining qualitative and quantitative habitat differences

Suppose that habitats along a gradient differ both quantitatively and qualitatively. Efficiency of resource acquisition along the gradient will be described by some function $E(x)$ and the shape of resource distribution along this gradient will be described by some function $R(x)$. (Each might be a Gaussian distribution, for example.) As in Model B, $RA(x) = kR(x)$, where k is a scaling constant for resource abundance. As in both other models, fitness (Φ) is a function of density (N), efficiency of resource acquisition (E) and resource abundance (R):

$$\Phi(N,E,R) = \gamma\left(kR(x) - N(x)\frac{p}{E(x)}\right)$$

Because efficiency and resource abundance are functions of position on the habitat gradient (x), fitness can also be described as a function of N and x. In Model C, fitness does decrease linearly with increasing N for each x_i. But, as resource abundance decreases, the fitness-density line becomes lower and steeper (Fig. 1C1 and 1C2). Owing to the ideal-free distribution, at any given time, Φ_i is a constant ($\Phi_i = \Phi_j = \phi$ for each i and j). For two time periods, 1 and 2, that differ in density–resource abundance ratio but not in the shape of $R(x)$:

$$\phi_1 = \gamma\left(k_1R(x) - N_1(x)\frac{p}{E(x)}\right)$$

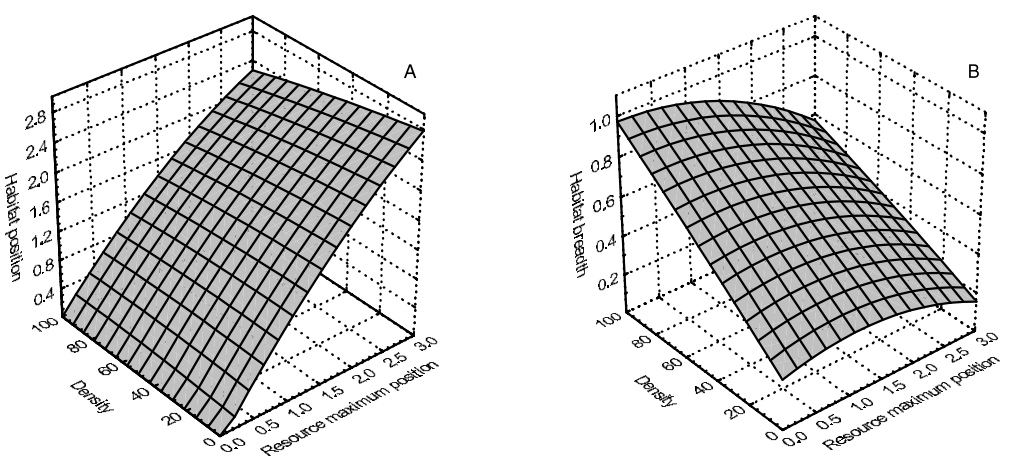

Fig. 3. The relationships between (A) density and habitat breadth and (B) density and position, as functions of the position of the resource abundance maximum in Model B.

$$\phi_2 = \gamma\left(k_2 R(x) - N_2(x)\frac{p}{E(x)}\right)$$

and

$$\gamma k_1 R(x) - N_1(x)\frac{\gamma p}{E(x)} - \phi_1 = \gamma k_2 R(x) - N_2(x)\frac{\gamma p}{E(x)} - \phi_2 = 0$$

$$N_2(x) = \frac{E(x)}{p}\left[k_2 R(x) - k_1 R(x) + \frac{\phi_1 - \phi_2}{\gamma}\right] + N_1(x)$$

Density relationships in Model C are not linear. To analyse the relationships between density and habitat breadth and position for the model, we used a numerical procedure. We assumed Gaussian distributions for both habitat quality and resource abundance with $(\sigma_E + \sigma_R)/2 = 1$. We set the bounds of the habitat gradient at -3σ and $+3\sigma$. Then we evaluated the model at 100 random points along the gradient.

The results show that the shape of the relationships between densities, habitat breadth and habitat position are determined by the positions of maxima of resource abundance and habitat quality. When both maxima coincide, each value of high density corresponds to one value of low density (Fig. 2C1). In this case, density relationships are almost equally well approximated by linear regression with a positive intercept (Fig. 4A) and by the non-linear regression $y = \sqrt{ax}$ (Fig. 4A). However, when the two maxima do not coincide, each value of high density corresponds to two different values of low density (Fig. 2C2). With moderate differences between resource abundance and efficiency maxima ($d < 1.5\sigma$), density relationships are better fitted by a non-linear regression ($y = \sqrt{ax}$) than by linear regression.

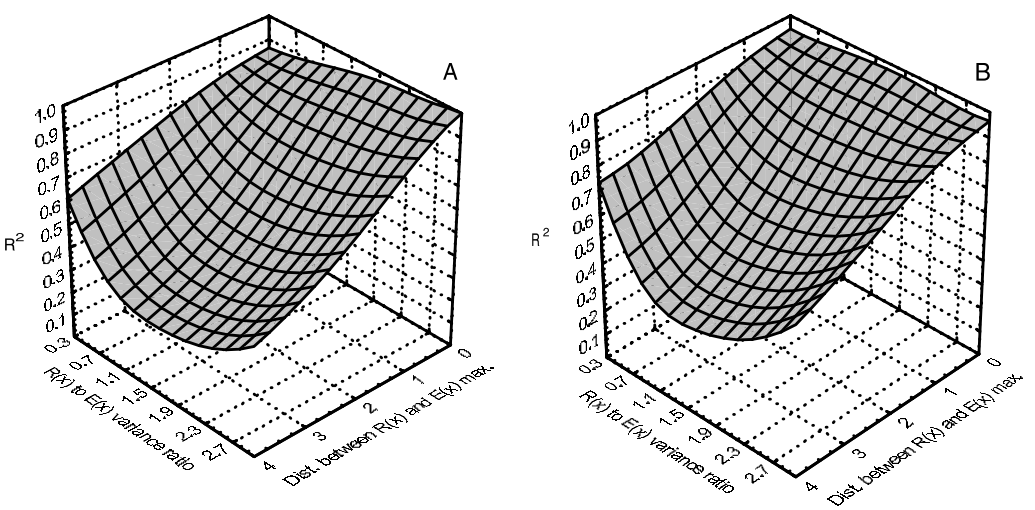

Fig. 4. Linear (A) and non-linear (B) quality of fit (R^2) of the density relationships (regression of low-density estimates against high-density estimates) depends on the positions of resource abundance and habitat quality maxima for Model C.

But if there are large differences between maxima ($d > 1.5\sigma$), then the density relationships do not fit any regression.

A habitat shift does not occur when both maxima coincide with the centre of the gradient, but does occur in the other cases. Habitat position shifts from the resource maximum at low density towards the centre of the gradient at high density. Moreover, the extent of this shift increases the further the centre of the gradient is from the value of the resource maximum (Fig. 5A). Habitat breadth increases with increasing density, and the rate of this growth decreases the further the resource maximum is from the centre of the gradient (Fig. 5B).

Predictions of these models are summarized in Table 1. Models B1 and C1 can be distinguished by regression analysis. Model B1 fits a linear equation ($y = a + bx$) better, whereas model C1 fits the non-linear form ($y = \sqrt{ax}$) better.

The paraisodar method depends on the assumption that every animal trapped in a plot lives there and uses it, and is neither a transient nor merely examining the habitat. If this assumption fails, we will find low densities even in rejected habitats. As a result, the true regression line could be biased, and the paraisodar may have a zero intercept (which will appear statistically like density-independent habitat selection) or fit the square root of a non-linear function. In addition, the prediction of a zero intercept is statistically untestable (because it is consistent with the null hypothesis). Both these problems can be partially avoided by a close examination of the scatter-plots and regression equations of the paraisodars.

APPLYING THE PARAISODAR METHOD TO SOME RODENT POPULATIONS

Material and methods

Study site

Ramon Canyon (30°35′N, 34°45′E, about 200 km^2 total area) forms the southern boundary of the Negev Highlands. Its northern and southern rims are 800 m and

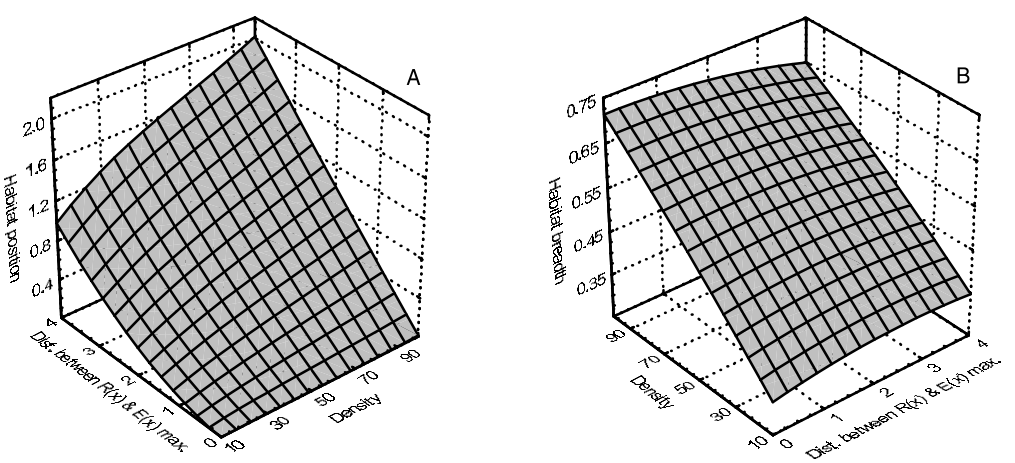

Fig. 5. The relationships between (A) density and habitat position and (B) density and habitat breadth depend on the distance between the resource abundance and habitat quality maxima for Model C.

Table 1. Summary of the predictions of models of habitat selection along an environmental gradient

Model	Conditions		Result	Indications			
				Linear regression parameters		Habitat change with density increase	
	Habitat quality	Resource abundance		Intercept	Slope	Breadth	Position
A	Constant shape of distribution	Constant	Density-independent habitat distribution	0	Positive	Stable	Stable
B1	Constant	Constant shape of distribution	Density-dependent habitat distribution	Positive	Positive	Increase	Stable
B2				Positive	Positive	Increase	Shift
C1	Constant shape of distribution	Constant shape of distribution	Density-dependent habitat distribution	Positive	Positive	Increase	Stable
C2				Non-significant	Non-significant	Increase	Shift

510 m above sea level respectively, and its lowest point is 420 m above sea level. Summer is hot and winter is relatively cool (mean monthly minimum and maximum air temperatures are 33.9°C and 19.7°C respectively in August, and 15.2°C and 6.6°C respectively in January). Rain usually falls from October to March. Annual rainfall declines sharply from 101 mm on the north rim of the canyon to 46 mm at its bottom (our data). There is a similar precipitation gradient from the west to the east in Ramon Canyon. Winter 1992–93 was dry (54% of mean annual precipitation), winter 1993–94 was moderately wet (115% of mean annual precipitation) and winter 1994–95 was wet (162% of mean annual precipitation).

The landscape of Ramon Canyon ranges from sand dunes to limestone to sandstone. Six main habitat types exist in the study area. They are characterized by their rodent species composition (Krasnov *et al.*, 1996).

- Sand dunes under the eastern wall of the canyon with *Calligonum comosum* or *Echiochilon fruticosum* (perennial vegetation cover, 7.4%)
- Flat gravel plains of the eastern part of the canyon with *Hammada salicornica*, *Anabasis articulata* and *Gymnocarpos decandrum* (cover, 5.7%)
- Limestone cliffs of the southern and central parts of the canyon with *Zygophyllum dumosum*, *Helianthemum kahiricum* and *Reaumuria hirtella* (cover, 4.0%)
- Wadis among rocky hills partially covered with loess over the northern rim of the canyon with *Anabasis articulata*, *Atriplex halimus* and *Artemisia herba-alba* (cover, 18.5%)
- Wadis of the eastern and central parts of the canyon with *Retama raetam*, *Moricandia nitens*, *Tamarix nilotica* and *Artemisia monosperma* (cover, 26.0%)
- Complex of narrow shallow wadis and loess hills of the western parts of the canyon with *Salsola schweinfurthii*, *Anabasis articulata* and *Atriplex leucocardia* (cover 6.0%).

Species of rodents

Twelve species form the community of desert rodents in Ramon Canyon: Dipodidae: *Jaculus jaculus* (Linnaeus, 1758) (67.0 g); Muridae: Gerbillinae: *Gerbillus dasyurus* (Wagner, 1842) (21.1 g), *Gerbillus gerbillus* (Olivier, 1801) (20.1 g), *Gerbillus henleyi* (de Winton, 1903) (9.8 g), *Gerbillus nanus* Blanford, 1875 (22.3 g), *Meriones crassus* Sundevall, 1842 (81.1 g), *Psammomys obesus* Cretzschmar, 1828 (166 g), *Sekeetamys calurus* (Thomas, 1892) (52.8 g), Murinae: *Acomys cahirinus* (Desmarest, 1819) (42.8 g), *Acomys russatus* (Wagner, 1840) (51.4 g), *Mus musculus* Linnaeus, 1758 (14.0 g); Myoxidae: *Eliomys melanurus* (Wagner, 1839) (49.6 g). Of these species, four (*A. cahirinus*, *A. russatus, M. musculus, E. melanurus*) are omnivorous, four (*G. dasyurus*, *G. gerbillus*, *G. henleyi*, *G. nanus*) are granivorous, one (*P. obesus*) is strongly folivorous, and three (*J. jaculus*, *M. crassus, S. calurus*) have a mixed diet of seeds and the green parts of vegetation.

Data collection

Rodents were trapped on 24 permanent 1-ha grids that were chosen to represent the main substrate and vegetation gradients. We set up the system of sampling grids beginning in summer 1992, and finishing in summer 1993. We began regular sampling of the grid system in July 1993 and continued to February 1996. We sampled both in winter (January–February) and in summer (July–August). We subdivided each grid into 25 plots of 20×20 m, with plot centres marked with numbered wire flags. Each trapped animal was sexed, weighed, marked by toe-clipping and released. We sampled each grid for 3 days using

50 Sherman folded live-traps placed near the centre of each plot. For bait, we used millet mixed with peanut butter. Jerboas are not trappable in live-traps in summer; we caught them with a net at night, using a search-light. *Psammomys obesus* are also not trappable in Sherman live-traps; we counted them in the morning with binoculars. We also mapped *Psammomys* burrows and then trapped *Psammomys* with Havahart two-door cage traps, model 1025 (two traps per burrow system), using fresh leaves of *Atriplex halimus* or succulent stems of *Anabasis articulata* as bait.

We took a 0.5-kg soil sample from the centre of each plot for laboratory texture analysis. We measured the angle of the slope of each plot with a clinometer. We counted the number of shrubs (by species) in each plot within a circle (5 m radius). To determine vegetation cover and volume by height layers within each plot, we measured the height and diameter of the crowns of the shrubs (up to 30 individuals of each species in the grid). We randomly placed four sample plots (0.25 m^2) in each plot and counted all annuals in them.

Altogether, 19 parameters were used in the subsequent analysis (Table 2). Descriptions of soil and shrub structure were made once at the beginning of the study (with redescription in a few cases where a severe winter flood modified the habitat structure of a plot). Descriptions of annual vegetation were made once each year just after the end of the winter trapping session. Summer annual plant abundance was not estimated because there are no summer annuals and winter annuals stop growing in April.

Statistical data processing

We divided each species' trapping sessions into two groups – low density (below average) and high density (above average). Within each group, we calculated average species density

Table 2. The 18 habitat variables in the analysis

Mnemonic	Variable	Units
SLP	Angle of the slope	degrees
RCK	Content of rocks in the soil	%
GRW	Content of gravel in the soil	%
CLY	Content of clay in the soil	%
FRB	Abundance of annual forbs	*n* per m^2
GRS	Abundance of annual grasses	*n* per m^2
GPH	Abundance of geophytes	*n* per m^2
CAR	Abundance of *Carex*	*n* per m^2
ANN	Overall abundance of annual grasses and forbs	*n* per m^2
MIC	Cover of microphyllous shrubs	%
APH	Cover of aphyllous shrubs	%
SUC	Cover of succulent shrubs	%
SCOV	Overall shrub cover	%
PGR	Perennial grass cover	%
SV1	Perennial plant crown volume at the level 0–25 cm	%
SV2	Perennial plant crown volume at the level 25–50 cm	%
SV3	Perennial plant crown volume at the level 0.5–1 m	%
SV4	Perennial plant crown volume at the level 1–2 m	%
SV5	Perennial plant crown volume at the level 2–4 m	%

for each grid. A data subset consisting of the grids with non-zero species densities at least in one of the two groups was extracted from the complete data pool. We estimated the parameters of linear regression for this data subset using low-density values as the independent variable and high-density values as the dependent variable. If the assumption of temporal stability of fitness–density relationships is correct, using averages instead of separate trapping session density estimates will produce the same type of regressions but with reduced error (due to the reduction in random deviations). If the results did not fit any of the models, we analysed the summer and winter trapping seasons separately.

Before we analysed habitat breadth and position, we log-transformed values of habitat variables to normalize them. To estimate values of habitat breadth, we subjected the data set – consisting of the values of habitat variables for each plot – to principal components analysis, and obtained scores of the principal component axes for each plot. Using projections of registration points on the component axes, we calculated coordinates of species centroids along each axis separately for low and high density. We measured habitat breadth as the standard deviation of observation points for a given species and density level from the centroid of that species in the space of the principal component axes.

To describe the distribution of species' spatial niches in the space of environmental variables (habitat space) and to reduce dimensionality of this space, we used discriminant analysis. With rodent species as a grouping variable, we calculated discriminant axes based on the data set, consisting of the values of habitat variables for each point of a rodent species' occurrence. Habitat position was represented as the coordinates of a species' centroid along each of the discriminant axes. Habitat shift was represented as the Euclidean distance between low- and high-density positions of species' centroids in discriminant space.

RESULTS

On the twenty-four 1-ha grids over four seasons, we obtained 3174 records of 1803 rodent individuals (278 records in summer 1993; 346 in winter 1994; 370 in summer 1994; 436 in winter 1995; 922 in summer 1995; and 822 in winter 1996). These data include 270 records of *J. jaculus*, 1456 *G. dasyurus*, 214 *G. gerbillus*, 232 *G. henleyi*, one *G. nanus*, 318 *M. crassus*, 359 *P. obesus*, 56 *S. calurus*, 84 *A. cahirinus*, 27 *A. russatus*, 147 *M. musculus* and 10 *E. melanurus*.

The low density of most gerbil and jird species occurred between the summer of 1993 and the winter of 1995. High densities for most species occurred in 1995 and in the winter of 1996 (Fig. 6). However, there were some exceptions. The high densities of *J. jaculus* occurred during the winter of 1994 and the winter of 1995; during other trapping sessions their density was low. The high density of *A. cahirinus* occurred in the summer of 1995; otherwise it was low. The high density of *A. russatus* occurred in the summers of 1994 and 1995; otherwise it was low. The density of *S. calurus* was constantly low during all periods. Very few *G. nanus* and *E. melanurus* were recorded and only in a minor subset of trapping sessions. We excluded the latter three species from the analysis. Habitat distribution of rodent densities during the periods of low and high density is presented in Table 3. There were two species with pronounced seasonal differences in habitat distribution, *J. jaculus* and *G. henleyi*.

Paraisodar analysis of the complete data sets (without taking into account seasonal differences in habitat distribution) showed (Table 4) that the linear regression with positive slope was statistically significant in most cases, with the exception of four species, *J. jaculus*,

Table 3. Habitat distribution of rodent densities during periods of low and high density

	Habitat types											
	Sand		Gravel plains		Eastern wadis		Cliffs		Loess hills		Western complex of wadis and hills	
Species	Low	High	Low	High	Low	High	Low	High	Low	High	Low	High
J. jaculus – summer	0.16	0.33	0.75	0.75	0.00	0.10	0.00	0.00	0.00	0.00	0.44	0.59
J. juculus – winter	0.33	0.33	0.62	0.88	0.50	0.50	0.00	0.00	0.00	0.00	0.67	0.92
E. melanurus	0.00	—	0.00	—	0.00	—	0.00	—	0.33	—	0.06	—
G. dasyurus	0.08	0.17	0.25	0.88	4.45	9.00	1.67	5.17	9.33	28.50	3.58	11.92
G. nanus	0.00	—	0.00	—	0.03	—	0.00	—	0.00	—	0.00	—
G. gerbillus	4.17	7.67	0.00	0.13	0.00	0.00	0.00	0.00	0.00	0.00	0.00	0.00
G. henleyi – summer	0.83	4.67	1.62	4.00	1.00	2.40	0.00	0.00	0.00	0.00	0.08	1.17
G. henleyi – winter	0.16	0.33	2.12	2.25	1.50	2.80	0.00	0.00	0.00	0.00	0.00	1.00
S. calurus	0.00	—	0.00	—	0.00	—	1.61	—	0.00	—	0.00	—
M. crassus	1.83	5.00	0.06	2.13	1.10	2.50	0.00	0.17	0.92	5.17	0.42	1.25
P. obesus	0.00	0.00	0.00	0.00	0.00	0.60	0.00	0.00	10.75	32.50	0.13	2.08
M. musculus	0.00	0.00	0.00	0.00	0.05	0.10	0.00	0.00	0.50	15.83	0.04	0.92
A. carhirinus	0.00	0.00	0.00	0.00	0.00	0.00	1.47	3.00	0.13	1.67	0.07	0.33
A. russatus	0.00	0.00	0.00	0.00	0.05	0.40	0.25	1.50	0.00	0.00	0.00	0.00

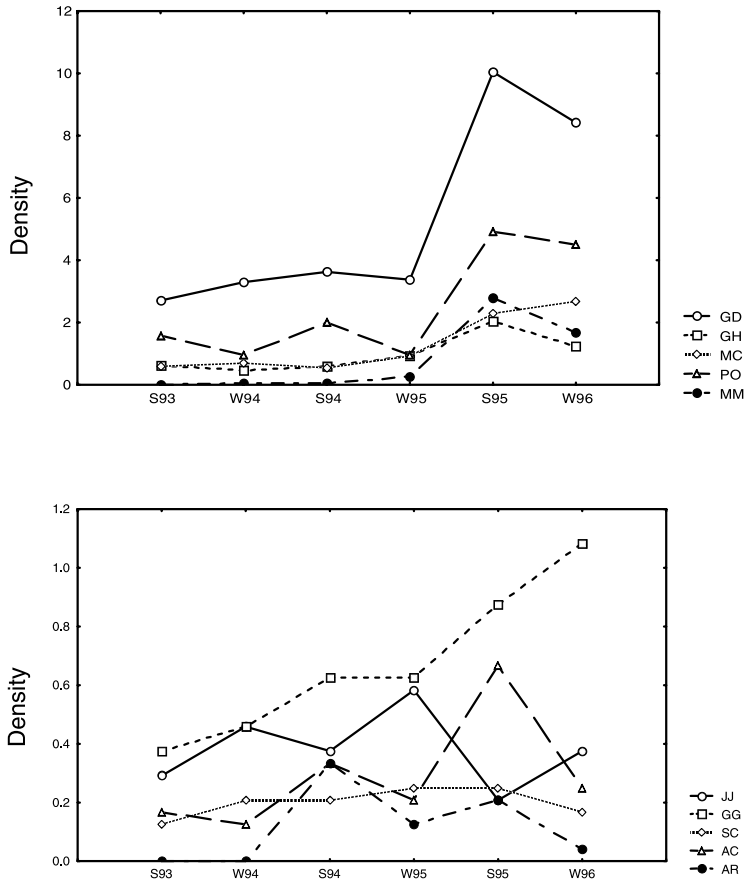

Fig. 6. Density (individuals per hectare) dynamics of rodents during the period of observations. S93 = summer 1993, W94 = winter 1994, S94 = summer 1994, W95 = winter 1995, S95 = summer 1995, W96 = winter 1996. Rodent species: AC = *Acomys cahirinus*, AR = *A. russatus*, GD = *Gerbillus dasyurus*, GG = *G. gerbillus*, GH = *G. henleyi*, JJ = *Jaculus jaculus*, MC = *Meriones crassus*, MM = *Mus musculus*, PO = *Psammomys obesus*, SC = *Sekeetamys calurus*.

G. henleyi, *M. crassus* and *A. cahirinus*. When we analysed summer and winter densities separately, the regression with a positive slope became significant also for *J. jaculus* in both seasons and for *G. henleyi* in winter. The regression intercept was significantly positive only in *M. crassus* and *A. russatus*. Non-linear regression ($y = \sqrt{ax}$) was significant in *G. dasyurus*, *G. gerbillus*, *G. henleyi* (in winter), *P. obesus* and *A. russatus*; in the latter two species, non-linear regression fits were better than the linear ones. However, visual inspection of scatter-plots (Fig. 7) reveals that the regression intercept is really close to zero only in *G. dasyurus*, *G. gerbillus* and *G. henleyi* in winter. In all other cases, the data are inadequate for precise estimation of regression intercepts.

The principal component analysis showed that the habitat variable space had five significant dimensions. These accounted for 77% of the variance (Table 5). These five axes reflected complex environmental gradients. The first axis represented an increase in the

Table 4. Summary of linear regression analyses between low and high density for each rodent species

	Linear regression ($y = a + bx$)			Non-linear regression ($y = \sqrt{ax}$)	
Species	Intercept ($a \pm$ S.E.)	Slope ($b \pm$ S.E.)	R^2	a	R^2
J. jaculus	0.483 ± 0.795	0.700 ± 0.711	0.069	1.426	0.032
J. jaculus – summer	0.333 ± 0.198	**0.738** ± 0.147	**0.661**	0.833	0.421
J. jaculus – winter	0.133 ± 0.598	**1.087** ± 0.294	**0.513**	1.363	0.364
G. dasyurus	–0.066 ± 3.567	**2.857** ± 0.245	**0.877**	48.22	**0.723**
G. gerbillus	1.056 ± 1.084	**1.542** ± 0.226	**0.959**	15.36	**0.944**
G. henleyi	1.902 ± 1.307	0.708 ± 0.362	3.360	6.015	0.310
G. henleyi – summer	2.536 ± 2.220	0.931 ± 0.589	0.173	9.645	0.443
G. henleyi – winter	0.896 ± 0.945	**0.978** ± 0.161	**0.804**	5.190	**0.589**
M. crassus	**1.907** ± 0.654	1.064 ± 0.695	0.117	9.960	0.026
P. obesus	8.281 ± 10.342	**2.170** ± 0.897	**0.661**	97.87	**0.714**
M. musculus	1.688 ± 5.634	**15.00** ± 4.517	**0.648**	237.6	0.510
A. cahirinus	0.673 ± 2.383	2.042 ± 1.219	0.319	7.954	0.187
A. russatus	**1.125** ± 0.306	**2.000** ± 0.500	**0.889**	5.008	**0.993**

Bold values represent $P < 0.05$.

Table 5. Principal component analysis of the habitats[a]

	PC1	PC2	PC3	PC4	PC5	PC6
Eigenvalue	6.623	3.184	2.027	1.417	1.325	0.934
Cumulative % of variance	34.86	51.62	62.29	69.74	76.72	81.73
			Factor loading			
SLP	–0.007	0.092	0.046	**–0.947**	–0.039	–0.083
RCK	–0.086	–0.061	**0.799**	–0.367	0.139	0.164
GRV	0.011	–0.249	**0.676**	0.293	–0.087	0.266
CLY	–0.146	0.130	0.131	0.232	**0.797**	–0.138
FRB	0.108	**0.860**	–0.184	0.096	0.111	0.267
GRS	0.052	**0.829**	0.001	–0.196	0.039	0.201
GPH	–0.157	0.063	**–0.637**	–0.128	0.365	0.369
CAR	–0.098	0.162	–0.208	–0.111	**0.749**	0.070
ANN	0.087	**0.898**	0.172	–0.014	0.172	0.271
MIC	0.211	0.093	0.056	0.030	0.057	**0.819**
APH	**0.822**	–0.046	0.038	0.045	–0.238	0.357
SUC	–0.239	0.462	0.044	–0.038	0.080	**0.577**
SCOV	0.384	0.298	0.064	–0.011	0.009	**0.831**
PGR	–0.076	0.046	**–0.564**	0.132	**–0.560**	0.050
SV1	0.249	0.340	–0.079	0.025	–0.100	**0.865**
SV2	0.420	0.282	0.067	0.112	–0.122	**0.814**
SV3	**0.694**	0.127	0.142	0.109	–0.121	**0.616**
SV4	**0.888**	0.095	0.059	0.052	–0.034	0.358
SV5	**0.882**	0.060	–0.066	–0.087	0.003	0.009

[a] PC1 to PC6 are the first six components. The first five are significant ($P < 0.001$). Mnemonics for habitat variables as in Table 2. **Bold** values represent factor loadings > 0.400.

abundance of tall aphyllous shrubs. The second axis reflected an increase in the abundance of annual vegetation. The third reflected an increase of rock and gravel content in the soil as well as a decrease of geophytes and perennial grasses. The fourth axis represented a decrease in the angle of slope. The fifth axis represented a gradient of increase of clay content in the soil and *Carex* abundance and a decrease in the abundance of perennial grasses.

Table 6 shows the values of habitat breadth measured in the principal component space. The complete data sets (without taking into account seasonal differences in habitat distribution) revealed that, as density increased, several species increased their habitat breadths significantly. These included *G. henleyi*, *M. crassus*, *P. obesus* and *A. russatus*. In contrast, *J. jaculus* decreased its habitat breadth significantly. The other species did not change their habitat breadths significantly with increasing density.

When summer and winter densities were analysed separately, no significant changes in habitat breadth with increasing density were found for *J. jaculus* in both seasons and for *G. henleyi* in winter. However, a significant increase of habitat breadth with density growth was recorded for *G. henleyi* in summer and for *A. cahirinus* in each trapping session (Fig. 7).

By reducing habitat space dimensionality using discriminant analysis, we showed that division of this space by the rodent community occurred mainly along the first three axes. These accounted for 89.5% of the variance. All three axes reflected some complex environmental gradients (Table 7). The first axis represented a general gradient of decrease of rock content in soil as well as an increase in the abundance of perennial grasses. The second axis reflected an increase of the angle of slope, and in the rock content of soil (with a parallel decrease of the clay and overall vegetation abundance). The third axis represented an increase of annual vegetation abundance (with a parallel decrease of the rock and gravel content in soil).

Table 6. Evaluations of habitat breadth and habitat shifts of rodent species at low and high density

	Habitat breadth			Habitat shift	
Species	Low density	High density	*t*-value	Distance	*t*-value
J. jaculus	1.535 ± 0.070	1.198 ± 0.037	4.256**	1.134 ± 0.352	3.222**
J. jaculus – summer	1.493 ± 0.148	1.507 ± 0.088	0.081	0.228 ± 0.571	0.399
J. jaculus – winter	1.331 ± 0.071	1.198 ± 0.037	1.661	0.314 ± 0.226	1.392
G. dasyurus	1.711 ± 0.029	1.654 ± 0.022	1.566	0.073 ± 0.132	0.552
G. gerbillus	1.130 ± 0.044	1.142 ± 0.059	0.163	0.240 ± 0.223	1.075
G. henleyi	1.442 ± 0.047	1.765 ± 0.067	3.947***	0.844 ± 0.247	3.417**
G. henleyi – summer	1.404 ± 0.066	1.798 ± 0.089	3.566**	1.112 ± 0.346	3.214**
G. henleyi – winter	1.462 ± 0.058	1.576 ± 0.085	1.458	0.508 ± 0.373	1.364
M. crassus	1.843 ± 0.050	2.045 ± 0.063	2.512*	0.729 ± 0.321	2.271*
P. obesus	1.259 ± 0.040	1.429 ± 0.031	3.359**	0.160 ± 0.256	0.625
M. musculus	1.176 ± 0.329	1.167 ± 0.035	0.027	0.502 ± 0.671	0.748
A. cahirinus	0.919 ± 0.060	1.133 ± 0.093	1.934	1.048 ± 0.449	2.332*
A. russatus	0.720 ± 0.186	1.607 ± 0.139	3.820***	0.129 ± 0.647	0.200

Significance of *t*-values: * $P < 0.05$, ** $P < 0.01$, *** $P < 0.001$.

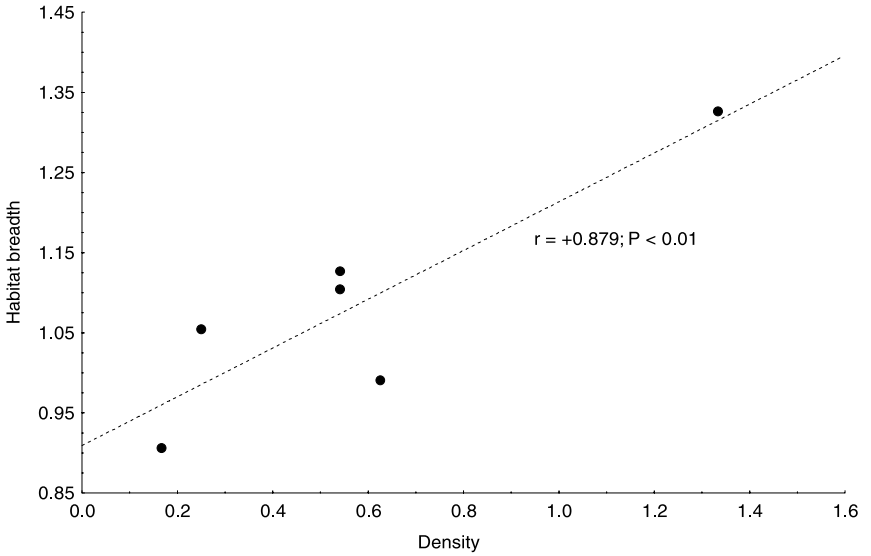

Fig. 7. Relationship between density (individuals per hectare) and habitat breadth in *A. cahirinus*.

General positions of all rodent species together in the space of the first two discriminant axes are presented in Fig. 8. Table 6 shows the values of habitat shift. Statistically significant habitat shifts with density change were recorded in three rodent species – *G. henleyi* (only in summer), *M. crassus* and *A. cahirinus*.

DISCUSSION

In several ways, our models correspond to those of Morris (1987, 1988, 1990) for 'one species/two habitat' systems. Model A makes the same predictions as Morris' divergent regulation model in qualitatively different but quantitatively identical habitats: density-independent habitat selection with linear density relationships and zero isodar intercepts. Model B makes the same predictions as Morris' parallel regulation model: density-dependent habitat selection with linear density relationships, positive isodar intercepts, and an increase in habitat breadth with density growth. Model C1 makes similar predictions to Morris' divergent regulation model in qualitatively and quantitatively different habitats: density-dependent habitat selection and an increase in habitat breadth with density growth. But the latter two models differ in the shapes of density relationships that they predict: these are linear in Morris' model and non-linear in ours.

Model C2 and Morris' crossover regulation model differ profoundly. They predict different trends of habitat breadth change: habitat breadth increases with increasing density in Model C2, but it decreases in Morris' model. We attribute these differences to the length of the habitat gradient, because we can obtain results similar to Morris' if we choose a very short gradient length (i.e. short relative to variability of resource abundance and variability of habitat quality). In any case, the reader should bear in mind that differences between our models and those of Morris are not contradictions because we are modelling different things.

Table 7. Discriminant analysis of the habitats of rodent species[a]

	DF1	DF2	DF3	DF4
Eigenvalue	1.111	0.716	0.379	0.119
χ^2	1982.3	1185.3	609.3	266.5
Cumulative % of variance	45.08	74.13	89.50	94.34
	Factor loading			
SLP	0.373	**0.570**	0.356	0.079
RCK	**0.704**	**0.338**	**–0.416**	–0.228
GRV	0.102	–0.029	**–0.598**	**–0.439**
CLY	0.389	**–0.423**	–0.305	**0.639**
FRB	0.175	**–0.569**	**0.431**	–0.254
GRS	0.397	**–0.405**	**0.599**	–0.001
GPH	–0.090	–0.163	0.254	0.165
CAR	0.223	–0.171	–0.032	0.479
ANN	0.255	**–0.519**	**0.464**	–0.170
MIC	0.245	–0.316	0.119	**–0.425**
APH	0.029	–0.142	0.087	–0.362
SUC	0.207	–0.237	0.109	–0.351
SCOV	0.265	**–0.401**	0.206	**–0.586**
PGR	**–0.412**	0.046	0.308	–0.232
SV1	0.181	**–0.415**	0.284	**–0.611**
SV2	0.220	**–0.440**	0.177	**–0.681**
SV3	0.209	–0.332	0.116	**–0.552**
SV4	0.203	–0.278	0.112	**–0.446**
SV5	0.125	–0.078	0.107	–0.324

[a] DF1 to DF4 are the first four components (all are significant, $P < 0.001$). Mnemonics for habitat variables as in Table 2. **Bold** values represent factor loadings > 0.400.

Among the nine rodent species, habitat selection in four fit the model predictions well. *Gerbillus dasyurus* and *G. gerbillus* fit Model A – density-independent habitat distribution. *Acomys russatus* fits Model C (variant 1) – density-dependent habitat selection with a constant shape of distribution of both resource abundance and habitat quality (and similar positions of maxima of resource abundance and habitat quality). *Meriones crassus* also fits Model C (variant 2 with distinct positions of resource abundance and habitat quality maxima).

In all other species, the data are inadequate for paraisodar analysis. However, putting together the results of the regression analysis and estimations of shifts in habitat position and habitat breadth, we can identify some additional cases of reasonable fit to the models (although these are far from ideal). One more species (*M. musculus*) fits Model A and another species (*P. obesus*) fits Model C1.

Two species with strong seasonal differences in habitat distribution (*J. jaculus* and *G. henleyi*) did not fit any model when the data of these seasons were pooled. However,

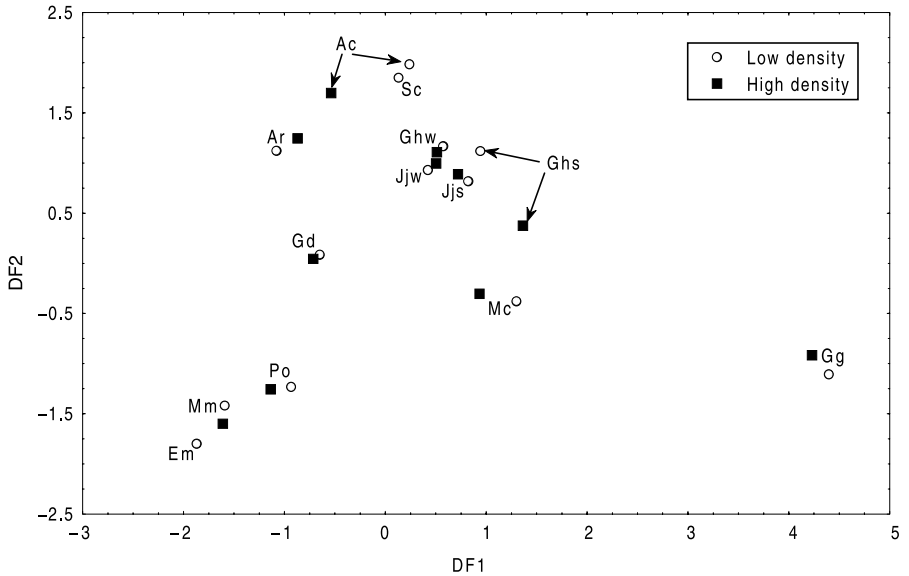

Fig. 8. Positions of species' habitat centroids in the space of the first two discriminant functions (DF1 and DF2) at low and high densities. Ac = *Acomys cahirinus*, Ar = *A. russatus*, Gd = *Gerbillus dasyurus*, Gg = *G. gerbillus*, Ghs = *G. henleyi* in summer, Ghw = *G. henleyi* in winter, Jjs = *Jaculus jaculus* in summer, Jjw = *J. jaculus* in winter, Mc = *Meriones crassus*, Mm = *Mus musculus*, Po = *Psammomys obesus*, Sc = *Sekeetamys calurus*. Arrows show statistically significant habitat shifts between periods of low and high densities.

separate analyses of summer and winter data revealed relatively good fits. *Jaculus jaculus* fits Model A in both seasons, and *G. henleyi* fits Model A in winter and Model C2 (variant 2) in summer. The latter result agrees with the pronounced seasonal differences in the biology of *G. henleyi* (Shenbrot *et al.*, 1994).

One species (*A. cahirinus*) also fits Model C (variant 2) – density relationships lack significance and habitat shift with density increase is significant. Increasing of habitat breadth with density in this species is revealed when analysing data of each trapping session separately, but not with pooled data in low-density seasons. This may be a result of hyper-dispersion (distribution of population over the landscape more even than random) in *A. cahirinus* (Abramsky *et al.*, 1985; Rosenzweig and Abramsky, 1985). In this case, a rapid increase in habitat breadth with density – even at low densities – produces an overestimate of habitat breadth in pooled data.

Our results differ somewhat from those of Abramsky *et al.* (1985) and Rosenzweig and Abramsky (1985), who studied these same species of Negev Desert rodents. They found density-dependent habitat selection in *G. gerbillus* and no indication of any habitat preferences in *G. dasyurus*. However, our paraisodar analysis indicates that both species are density-independent habitat selectors. The discrepancy in *G. dasyurus* may result from a difference in the range of habitats considered. Abramsky *et al.* (1985) and Rosenzweig and Abramsky (1985) analysed the spatial distribution of *G. dasyurus* only within rocky habitats, whereas we looked at the whole habitat spectrum. The discrepancy in the *G. gerbillus* results may reflect geographical variability in habitat selection. Whereas Abramsky *et al.* (1985)

and Abramsky and Rosenzweig (1985) studied populations of *G. gerbillus* in places where it co-exists with potential congeneric competitors (*G. allenbyi* and *G. pyramidum*), the population we studied is a small peripheral isolate that occurs in the absence of any potential congeneric competitor (Krasnov *et al.*, 1996).

Among the nine rodent species we studied, four are density-dependent habitat selectors, four are density-independent habitat selectors, and one is a density-dependent habitat selector in summer and a density-independent habitat selector in winter. It may be interesting to obtain data on the ratio of density-dependent and density-independent species in other communities. Differences in this ratio can create different patterns of temporal community dynamics.

ACKNOWLEDGEMENTS

This work was supported by a special grant for immigrant scientists of the Ministry of Science and Art of the State of Israel. We thank Z. Abramsky, B. Kotler and D. Ward (all of Ben-Gurion University of the Negev) for their helpful comments on the manuscript. We also thank D.W. Morris (Center of Northern Studies, Thunder Bay, Canada) for fruitful discussions on the manuscript. This is publication No. 52 of the Ramon Science Center.

REFERENCES

Abramsky, Z., Rosenzweig, M.L. and Brand, S. 1985. Habitat selection of Israel desert rodents: Comparison of a traditional and a new method of analysis. *Oikos*, **45**: 79–88.

Fretwell, S.D. and Lucas, H.L., Jr. 1970. On territorial behavior and other factors influencing habitat distribution in birds. I. Theoretical development. *Acta Biotheor.*, **19**: 16–36.

Krasnov, B., Shenbrot, G., Khokhlova, I. and Ivanitskaya, E. 1996. Spatial patterns of rodent community in the Ramon Erosion canyon, Negev Highlands (Israel). *J. Arid. Environ.*, **32**: 319–327.

Morris, D.W. 1987. Ecological scale and habitat use. *Ecology*, **68**: 362–369.

Morris, D.W. 1988. Habitat-dependent population regulation and community structure. *Evol. Ecol.*, **2**: 253–269.

Morris, D.W. 1990. Temporal variation, habitat selection and community structure. *Oikos*, **59**: 303–312.

Rosenzweig, M.L. 1974. On the evolution of habitat selection. In *Proceedings of the First International Congress of Ecology*, pp. 401–404. Wageningen, The Netherlands: Centre for Agricultural Publishing and Documentation.

Rosenzweig, M.L. 1981. A theory of habitat selection. *Ecology*, **62**: 327–335.

Rosenzweig, M.L. 1989. Habitat selection as a source of biological diversity. *Evol. Ecol.*, **1**: 315–330.

Rosenzweig, M.L. 1991. Habitat selection and population interactions: The search of mechanism. *Am. Nat.*, **137**: 5–28.

Rosenzweig, M.L. 1995. *Species Diversity in Space and Time*. Cambridge: Cambridge University Press.

Rosenzweig, M.L. and Abramsky, Z. 1985. Detecting density-dependent habitat selection. *Am. Nat.*, **126**: 405–417.

Shenbrot, G.I. and Rogovin, K.A. 1995. Temporal variation in spatial organization of a rodent community in the southwestern Kyzylkum Desert (Middle Asia). *Ecography*, **18**: 370–383.

Shenbrot, G., Krasnov, B. and Khokhlova, I. 1994. On the biology of *Gerbillus henleyi* (Rodentia: Gerbillidae) in the Negev Highlands, Israel. *Mammalia*, **58**: 581–589.